Towards practical biomolecular computers using microfluidic deoxyribozyme logic gate networks

Joseph Farfel jfarfel@cs.unm.edu
Darko Stefanovic darko@cs.unm.edu
Department of Computer Science
University of New Mexico

Abstract

We propose a way of implementing a biomolecular computer in the laboratory using deoxyribozyme logic gates inside a microfluidic reaction chamber. We build upon our previous work, which simulated the operation of a deoxyribozyme-based flip-flop and oscillator in a continuous stirred-tank reactor (CSTR). Unfortunately, using these logic gates in a laboratory-size CSTR is prohibitively expensive, because the reagent quantities are too large. A desire to reduce the cost of open-reactor experiments using these gates motivated our decision to design a microfluidic system. For a realistic microfluidic design, the properties of microfluidic flow and mixing have to be taken into account. We describe the differences between a macrofluidic system such as the CSTR and a microfluidic setting. Liquid in a microfluidic setting exhibits laminar flow, and is more difficult to mix than in a CSTR. We would like to use a rotary mixer, and so we examine how it operates so that we may properly model it. We discuss the details of our mixer simulation, including our diffusion model. We discuss why having discrete phases of influx/efflux ("charging") and mixing is necessary, and how it changes the kinetics of the system. We then show the result of simulating both a flip-flop and an oscillator inside our rotary mixing chamber, and discuss the differences in results from the CSTR setting.

1 Introduction

Deoxyribozymes (nucleic acid enzymes) may be used as logic gates, which transform input signals, denoted by a high concentration of substrate molecules, into output signals, which are represented by product created when the deoxyribozyme gate cleaves a substrate molecule [1]. Using these gates, molecular devices have been created in the laboratory that function as a half-adder [2] and a tic-tac-toe automaton [3]. Furthermore, experiments have demonstrated the linking of the output of certain deoxyribozyme gates to the input of others, which opens the prospect of creating complex logic [4].

These gates have so far only been used in the laboratory in very small quantities, and, quite significantly, only in closed reactors. This is due to the expense that inhibits purchasing large amounts of gate molecules and the substrates that act as their input. Using these gates in closed reactor systems has the major drawback of limiting them to performing one-shot computations. Previously, we have simulated multiple gate operation in an open, continuous-influx stirred tank reactor (CSTR), and have shown designs for a flip-flop and an oscillator in this setting [5]. Unfortunately, no such open reactor experiment has been performed, owing to the attendant costs.

We propose a microfluidic system whereby these open reactor experiments may actually be performed in the laboratory at a modest cost in materials and apparatus. We analyze and simulate a molecular flip-flop and oscillator in a microfluidic setting. The reaction kinetics of the flip-flop and oscillator in the CSTR have already been examined in detail. Our simulation changes these kinetics by making the influx and homogeneity of the system time-dependent, varying according to our simulation of a microfluidic mixer, which doubles as the reaction chamber.

The extremely small volume of a microfluidic reaction chamber (ours is 7.54 nL) compared to a CSTR (50 mL or more) means that the same or even substantially greater concentrations of oligonu-

cleotide gates and substrates can be obtained within the chamber even with a vastly smaller amount of gate and substrate molecules. This means that the expense of an open-reactor experiment (mostly determined by the amount of substance used—including the substrates, the products, and the gates) can be reduced by several orders of magnitude, and be made reasonable. The initial cost of building the microfluidic system may be large, but the benefit of being able to run experiments with a very small number of pricey deoxyribozyme molecules far outweighs this initial investment. In addition to reducing expense and thereby enabling real-life open-reactor experiments, this approach has numerous other advantages unique to a microfluidic system, including a vast decrease in the time needed to perform logic operations, the possibility of keeping gates inside a chamber (allowing for pre-fabricated chambers, each implementing a certain type of logic), and the ability to link reaction chambers together with externally-controlled valves. Linking chambers together could allow us to create complex networks of reaction chambers, and channels between chambers could even be designed to mimic capillaries connecting living cells in which computation may be taking place *in vivo* at some point in the future. In fact, we consider this microfluidic setting to be the proving ground for deoxyribozyme logic gate circuits for medical applications.

2 The Chemical Kinetics of Deoxyribozyme Gate Networks

The four chemical components present in our reactor are inputs, gates, substrates, and products. All of these components are oligonucleotides. The gates are deoxyribozyme molecules, and under certain input conditions they are active [1]. When a gate becomes active, it cleaves substrate molecules to create product molecules. In more technical terms, the enzymatic (active) gate is a phosphodiesterase: it catalyzes an oligonucleotide cleavage reaction. Input molecules can either activate or deactivate a gate. The effect that a particular type of input molecule has on a gate defines its function. For instance, a simple inverter, or NOT gate, will be active, and cleave substrate to produce product, until an input molecule binds to it, making it inactive. The concentration of product in the system is the output signal of the gate, where a high concentration of product is read as true and a low concentration is read as false (the same is true for high or low input concentrations). Product molecules fluoresce, while substrate molecules do not, so the concentration of product molecules in the system is determined by the level of emitted fluorescence. For the NOT gate example, the concentration of product in the system becomes high when there is no input and becomes low when input molecules are added, as the input molecules deactivate all of the gate molecules and product is no longer being cleaved from substrate. This example of the NOT gate's operation depends on its being in an open reactor, however—if it is in a closed reactor, the product concentration can never go from high to low, but in an open reactor, product is always being removed from the system as part of the system's efflux.

In order to model the operation of these logic gates, we must be well informed of their basic chemical kinetics. The kinetics of the YES gate have been thoroughly examined [5], and we use those results here. In this examination, it is assumed that the bonding between gate and input molecules is instantaneous and complete, since it is known that the cleavage and separation of the substrate molecules into product molecules is the slowest of the reactions, and thus is the rate-limiting process. The rate at which product is produced by a gate is $\frac{dP}{dt} = \beta S G_A$, where P is the product concentration, β is the reaction rate constant, S is the substrate concentration, and G_A is the concentration of active gates. It has been empirically determined that the reaction rate constant for the YES gate is approximately $\beta = 5 \cdot 10^{-7}\ \mathrm{nM}^{-1}\mathrm{s}^{-1}$. This value will be assumed as the reaction rate for all deoxyribozyme gates mentioned herein.

The chemical kinetics of an entire system of gates, substrates, inputs, and products in an open, microfluidic reactor can be modeled with a set of coupled differential equations. An example is the case of the inverter, or NOT gate, where the set of equations is:

$$\frac{dG}{dT} = \frac{G^m(T) - E(T)G(T)}{V}$$

$$\frac{dI}{dT} = \frac{I^m(T) - E(T)I(T)}{V}$$

$$\frac{dP}{dT} = \beta H(T)S(T)\max(0, G(T) - I(T)) - \frac{E(T)P(T)}{V}$$

$$\frac{dS}{dT} = \frac{S^m(T)}{V} - \beta H(T) S(T) \max(0, G(T) - I(T)) - \frac{E(T)S(T)}{V}$$

where I^m, G^m, and S^m are the rates of molar influx of the respective chemical species, V is the volume of the reactor, $E(T)$ is the rate of volume efflux, β is the reaction rate constant, and $H(T)$ is a number representing the volume fraction of the reaction chamber that is homogeneous at time T. The influx and efflux of the reactor are time-dependent, because the reactor must close off its input and output periodically in order to mix its contents (*vide infra*). The variable $H(T)$ is needed because in a microfluidic system we cannot assume that the contents of the reactor are always perfectly mixed. New substrate that comes into the system during the period of influx must be mixed before it may react with the gates in the system. This allows for separate influx streams for new gates and for substrates and input molecules. It also allows for the possibility that new gates never enter or leave the system at all; instead, they could be attached to beads which cannot escape semi-permeable membranes at the entrances and exits to the chamber. In either case, only that portion of the total substrate in the chamber that has been mixed with the solution containing the gates may react. The specifics of how the efflux and the homogeneity of the system are calculated are discussed in the next two sections.

3 Microfluidics

In order to simulate an open microfluidic reaction system, we must first analyze the properties of such a system. First, and most obviously, the size of a microfluidic reaction chamber is dramatically small compared to the size of a more conventional open reaction chamber, such as a CSTR. The volume of the smallest CSTR that can be readily assembled is on the order of 50 mL (our previous work used 500 mL), while the volume of a microfluidic reaction chamber is often on the order of 5 nL—a difference of seven orders of magnitude. The reaction chamber we chose for our simulation has a volume of 7.54 nL. This very small volume allows us to have very high concentrations of gate, substrate, input, and product molecules, while keeping the actual number of molecules in the system low.

Fluid flow in microfluidic channels and reaction chambers is different from the flow in a large-scale system because of the very small volumes involved. Namely, the flow is laminar, i.e., there is no turbulence (the Reynolds number of the flowing liquids is typically well below 100). This presents a peculiar challenge: two fluids flowing side by side in a microfluidic channel do not mix except by diffusion, which is a very slow process, but the fluid already in an open reaction chamber must mix quickly with new fluid flowing into the chamber, which contains new supplies of substrates, inputs, and gates, to allow the reaction to continue. This necessitates the use of an active microfluidic mixer for our reaction chamber, to speed up the mixing of the fluids greatly over normal mixing by diffusion.

We have chosen a microfluidic rotary pump to act as our open reaction chamber [6]. This device is an active mixer, mixing the solution within it by pumping it in a circular loop. The design of the device is shown in Figure 1. It consists of a bottom layer with fluid channels, and a top layer with pneumatic actuation channels. Both layers are fabricated with multilayer soft lithography [7]. One input channel in the bottom layer is used for substrate and input influx, while the other channel is used for gate influx—this separation is to keep the substrate and gates from reacting before they have entered the reaction chamber. The pneumatic actuation channels on the top layer form microvalves wherever they intersect with the fluid channels on the bottom layer. A valve is closed when an air channel is pressurized and open when it is not. The actual reaction chamber is the central loop in the diagram. Actuating the valves around the perimeter of the loop in a certain sequence peristaltically pumps the fluid inside either clockwise or counterclockwise. The frequency of actuation controls the speed at which the fluid rotates.

Continuous-flow mixing is possible with this reaction chamber [6], but it is not feasible for our purposes for two reasons. The first is that the mixer does not completely mix objects with relatively low diffusion constants, such as very large molecules and 1 μm beads, when the flow is continuous. An experiment was performed [6] in which there was a continuous flow through the mixer of one solution containing dye and another solution containing beads. The two solutions entered the mixer side by side in the entrance channel, flowing laminarly. In the fluid

exiting the mixer, the dye was completely mixed, but only one quarter of the beads had crossed over to the other side of the fluid channel. Even if sufficient mixing of oligonucleotide molecules of the size we currently use could be achieved by using a low flow rate or widening and lengthening the mixer loop, this is not conducive to the possibility of attaching gates to beads, so that they may be kept always in the chamber by using semi-permeable membranes. The second problem is that the flow rate required for continuous-flow operation would have to be unreasonably low, in order to allow the gates involved to produce product molecules faster than they are removed from the system. Therefore, our model of the rotary mixing chamber uses two discrete, alternating phases: an influx and efflux, or "charging" phase, during which the valves at the chamber entrance and exit are open and the rotary pump is not operating, and a mixing phase, during which the valves at the entrance and exit of the chamber are closed and the pump is operating.

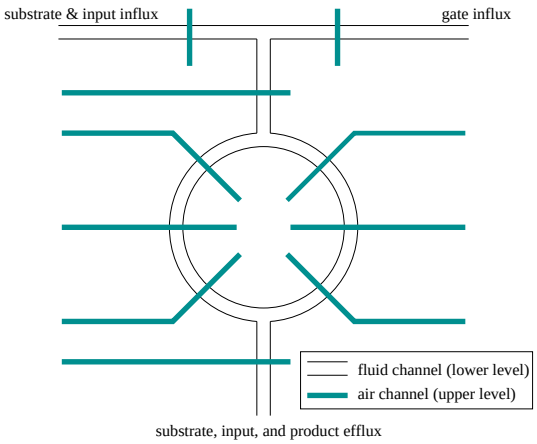

Figure 1: The rotary mixer. The air channels form microvalves wherever they intersect with the fluid channels.

4 Mixing and Diffusion

Through a combination of factors, the rotary pumping in the mixing chamber greatly increases mixing speed compared to spontaneous diffusion. The time it takes to mix fluids is not negligible, however, and so we must examine how it works, and model its operation in our micro-system simulation. The parabolic flow profile present in microfluidic channels (the fluid in the middle moves much faster than the fluid on the very edge, which is stationary) causes interface elongation, which, combined with the shallow channel depth, causes the mixing substances to fold around one another [6]. Where once the two fluids being mixed were completely separated, one in one half of the chamber and the other in the other half, after sufficient mixing time the width of the channel holds many alternating sections ("folds") of the two fluids. The two fluids still mix via diffusion, but folding them around each other greatly reduces the distance across which molecules from one fluid must diffuse into the other.

We can think of a substance as being completely homogeneous in the chamber when enough of that substance has diffused, from the fluid it was in originally, across a characteristic distance l, which is the farthest the substance must penetrate into the second fluid. Initially, we have $l_0 = r_0$, where r_0 is half the width of the channel that forms the mixing chamber. This is because we can assume that initially, when there is perhaps one fold in the chamber, the two liquids are side by side, with one liquid filling up half of the channel and the other filling up the other half. In order for a substance to be completely mixed in this situation, it must diffuse from its liquid all the way across half the width of the channel, until it reaches the far edge of the second solution at the chamber's wall. As the mixer continues running, however, the characteristic distance over which the fluids must diffuse to mix is reduced proportionally to the number of rotations, because of the liquids' folding around each other. Specifically, we have $l = l_0/kt$, where k is a constant coefficient determined by the total length of the loop and the pumping speed [6].

Knowing how the maximum characteristic diffusion distance changes over time, it is possible to model the mixing of the system using a diffusion equation. We use an equation which models diffusion of a substance in a fluid that is extended in all dimensions, where the substance is initially confined in one dimension in the region $-h < x < +h$. The regions from $-h$ to $-\infty$ and from $+h$ to $+\infty$ contain fluid with zero initial concentration of the diffusing substance. The substance is free to diffuse in either direction—solutions may be found for negative and

positive values of x. The equation is:

$$C(x,t) = \frac{1}{2}C_0\left\{\text{erf}\frac{x-h}{2\sqrt{Dt}} + \text{erf}\frac{x+h}{2\sqrt{Dt}}\right\}$$

where $C(x,t)$ is the concentration of the diffusing substance at location x and time t, C_0 is the concentration initially within the region $-h < x < +h$, D is the diffusion constant of the diffusing substance, and erf is the standard mathematical error function ($\text{erf}\, z = \frac{2}{\sqrt{\pi}}\int_0^z \exp(-\eta^2)d\eta$) [8]. Because the liquids are folding around each other, both h, which bounds the fluid the substance must diffuse out of, and the farthest distance $x = h + l$ to which it must diffuse, are time-dependent. We already know that $l = l_0/kt$, and, since we shall assume that the two fluids have equal-size folds at any given time t, we know that $h = l$.

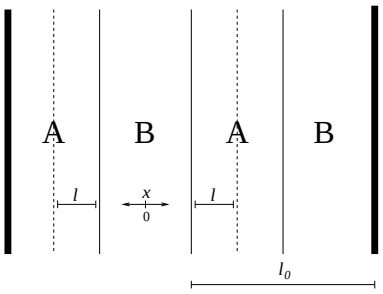

Figure 2: Folds in a section of the mixer channel.

The only problem with using these equations to model our rotary mixer is that we do not know what the constant k is in the equation for the length of diffusion l. We do know, however, from empirical evidence [6], that at a certain pumping speed it takes 30 seconds to completely mix a solution containing dye with a solution containing 1μm beads. We can use this fact to estimate k by noting the value of k for which the concentration of diffusing beads at the maximum mixing distance l is approximately equal to the concentration of beads in the middle of the fluid containing them originally (at $x = 0$) at time $t = 30$ s. Conservatively, we choose to focus on the beads for determining when the fluids are completely mixed because they have a diffusion constant that is much lower than the dye, and thus they diffuse much more slowly. The diffusion constant of the beads is $D = 2.5 \cdot 10^{-9}\,\text{cm}^2\text{s}^{-1}$. We find that the concentrations are 97.72% the same when $k = 2$. We do not attempt to get the concentrations to be 100% equivalent, because we realize that the diffusion equation becomes less accurate at the boundary condition at the end of the mixing process, since it assumes that the fluid extends infinitely and substance does not diffuse completely during the duration of the experiment. Also, it is much safer for our purposes to underestimate k than overestimate it, as an underestimate leads to slower mixing, which has the potential to disrupt the kinetics of our chemical system. We shall see, however, that it does not disrupt it enough to cause the logic that the gates perform to break down.

Using our value of $k = 2$, and the equations for the characteristic length of diffusion and the concentration of a diffusing substance at time t and position x, we can simulate the mixing chamber. There are no beads involved in our experiments; rather, we are only mixing fluids with gate, substrate, and input molecules. So, in accordance with the length of our oligonucleotide strands, we use the diffusion constant for a DNA 50-mer, which is $1.8 \cdot 10^{-7}\,\text{cm}^2\text{s}^{-1}$, in our mixing simulation. The mixing affects the differential equations describing the kinetics of the chemical system within the chamber by way of $H(T)$, which is a function of time (see Section 2). This function returns the fraction of the reaction chamber which is mixed. As noted earlier, during an experiment the rotary mixer alternates spending time in a charging phase, where there is an influx of new substrate, input, and gate molecules and an efflux of homogeneous solution, and a mixing phase, where the influx and efflux valves are closed and the rotary pump is turned on.

5 A Flip-Flop

Now that we can model the microfluidic mixing chamber, we must implement interesting logic in it using networks of deoxyribozyme-based logic gates. Since we are using an open system, we can create circuits which have persistent information that can be accessed and changed over time. The simplest such digital circuit is the *flip-flop*. A flip-flop is a bistable system which represents a single bit of memory. It can be commanded to *set* or *reset* this bit, which

causes it to enter its high or low stable state, respectively, or to simply store, or *hold*, the bit in memory, in which case it stays in the state that it was last set or reset to.

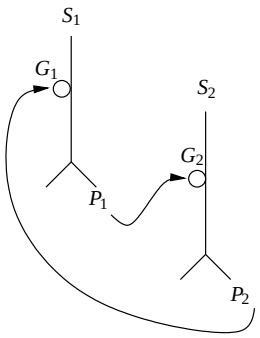

Figure 3: The flip-flop reaction network.

We simulated the operation of a biochemical flip-flop within our modeled microfluidic mixing chamber. The flip-flop was implemented as a network, shown in Figure 3, of two deoxyribozyme-based NOT gates connected in a cycle of inhibition [5]. In this system there is no influx of input molecules, only of substrate molecules. We use the substrate molecules themselves to control the behavior of the flip-flop. A high concentration of substrate S_2 signifies a set command; a high concentration of substrate S_1 signifies a reset command; and a high concentration of both substrates is used as the hold command. The first gate, G_1, can only cleave substrate S_1, and produces product P_1. The product P_1, in turn, acts as the input molecule for the second NOT gate, G_2, inhibiting its operation. When there is little or no P_1, the second gate G_2 is active, and it cleaves substrate S_2 to produce product P_2, which acts to inhibit the operation of the first gate, G_1. We measure output from the flip-flop in terms of the concentration of the cleaved product P_2, with high or low concentrations corresponding to a logical one or zero, respectively. It is apparent that the commands of set, reset, and hold we mentioned earlier will perform correctly with this inhibition cycle, with certain parameters. If only substrate S_1 is present in the system, only product P_1 and no P_2 will be produced—this corresponds to the reset command. If only S_2 is in the system, only product P_2 will be produced—this corresponds to the set command. However, if both S_1 and S_2 are in the system, we will stay at whatever state we were at previously, because whichever gate was originally producing more product than the other will inhibit the operation of the other gate, and will itself become less inhibited as a result, and thus eventually will become the only operating gate—this corresponds to the hold state. This operation requires that the concentrations of the gates are equal, for symmetry, and also that the efflux of the system is not greater than the rate at which the gates can produce product, so product is not being removed faster than it is being created.

The details of this bistable flip-flop system in a CSTR were examined thoroughly in previous work [5]. In the case of implementing this gate network in a microfluidic rotary mixer, we first define $S_1^m(T)$ and $S_2^m(T)$ to be the variable *molecular* influx of the substrates at time T, with which the flip-flop is controlled. The variable molecular influx of gate molecules, which enter the reactor in a separate stream from the substrate and input molecules, is given by $G_1^m(T)$ and $G_2^m(T)$. The rate of efflux is given by $E(T)$, and is time-dependent, because the system only has influx and efflux during its charging phase, and not during its mixing phase. We define $G_1(T)$, $G_2(T)$, $P_1(T)$, $P_2(T)$, $S_1(T)$, and $S_2(T)$ to be the concentrations within the reactor at time T of gate 1, gate 2, product 1, product 2, substrate 1, and substrate 2, respectively. We can now represent the dynamics of the flip-flop system with a set of six coupled differential equations:

$$\frac{dG_1}{dT} = \frac{G_1^m(T) - E(T)G_1(T)}{V}$$

$$\frac{dG_2}{dT} = \frac{G_2^m(T) - E(T)G_2(T)}{V}$$

$$\frac{dP_1}{dT} = \beta_1 H(T) S_1(T) \max(0, G_1(T) - P_2(T)) - \frac{E(T)P_1(T)}{V}$$

$$\frac{dP_2}{dT} = \beta_2 H(T) S_2(T) \max(0, G_2(T) - P_1(T)) - \frac{E(T)P_2(T)}{V}$$

$$\frac{dS_1}{dT} = \frac{S_1^m(T)}{V} - \beta_1 H(T) S_1(T) \max(0, G_1(T) - P_2(T)) - \frac{E(T)S_1(T)}{V}$$

$$\frac{dS_2}{dT} = \frac{S_2^m(T)}{V} - \beta_2 H(T) S_2(T) \max(0, G_2(T) - P_1(T)) - \frac{E(T)S_2(T)}{V}$$

where β_1 and β_2 are the reaction rate constants, V is the volume of the reactor, and $H(T)$ is the fraction of the substrate molecules in the chamber which have been mixed (these are the only ones available to react).

In order to achieve flip-flop behavior with this system, we must find appropriate values for the system's

efflux, the mixing rate, and the time spent by the system in its mixing phase and charging phase. We fix our mixer's high efflux at $0.12\,\mathrm{nL\,s^{-1}}$. During the charging phase, the mixer has this high efflux value, while during the mixing phase, the efflux is 0. The influx of the mixer is the same as the efflux, to maintain constant volume. We fix the mixing rate based on our empirically determined value for the constant k, which directly controls the mixing speed by determining the number of folds the mixer produces in a given amount of time. This value could be significantly adjusted in reality, as k simply depends on the length of the mixing channel and the speed of the pumping; our value of $k = 2$ reflects what we have determined to be one realistic value. With the efflux and mixing rate fixed, the only variable affecting the operation of the flip-flop is the time the mixing chamber spends in its charging and mixing phases. We find empirically that it works very well to spend 15 seconds in the charging phase and 15 seconds in the mixing phase.

With these parameters, Figure 4 shows the system of equations numerically integrated over a period of $1.2 \cdot 10^4$ s. The concentration of each type of gate molecule in the chamber was held steady at 130 nM, with the molecular influx of gates always matching the efflux of gates. We move the system from set, to hold, to reset at $2.5 \cdot 10^3$ s intervals. The rapid, shallow oscillations in product concentration are due to the alternating, discrete sections of charging and mixing the system experiences.

Figure 5 shows the flip-flop switching between the set and reset commands at its maximum rate of speed. This rate was determined in our simulation to be about 900 seconds given to each command. This is over 65 times faster than simulations showed the flip-flop's maximum switching rate to be in the CSTR. We should also note that the concentration of substrate within the reaction chamber is a factor of 10 higher than in the CSTR simulation. Because the volume of our mixing chamber is over 7 orders of magnitude smaller than the volume of the CSTR, however, and our flow rate is 5 orders of magnitude lower, the total number of moles of substrate used in the microfluidic simulation is vastly lower than in the CSTR simulation. In fact, the molecular influx of a high substrate signal is only about $7.29\,\mathrm{fmol\,s^{-1}}$. Thus, in the span of a 1.2×10^4 s experiment (a little over three hours), less than two tenths of a nanomole of substrate is used.

6 An Oscillator

If we increase the number of enzymatic NOT gates in our microfluidic reaction chamber to any odd number greater than one, we can create a biochemical oscillator. We will focus on a network of three NOT gates for simplicity. The three gates are, as before, connected in a cycle of inhibition. We require three different substrates, one matching each gate. Each gate cleaves its substrate into a unique product which inhibits one other gate. Gate G_1 cleaves substrate S_1 to produce product P_1, which acts as input to gate G_2, inhibiting it, while gate G_2 cleaves S_2 to produce P_2, which inhibits gate G_3, and finally gate G_3 cleaves the substrate S_3 to produce P_3, which inhibits gate G_1. As before, there will be one input stream which is a mixed solution containing the three types of substrate molecules, and another stream containing fresh gate molecules. The output of the system will be a solution containing only substrate and product molecules.

We define $G_1(T)$, $G_2(T)$, $G_3(T)$, $S_1(T)$, $S_2(T)$, $S_3(T)$, $P_1(T)$, $P_2(T)$, and $P_3(T)$ to be the concentrations within the reactor at time T of the gates, substrates, and products. We define $G_1^m(T)$, $G_2^m(T)$, $G_3^m(T)$, $S_1^m(T)$, $S_2^m(T)$, and $S_3^m(T)$ to be the molecular influx rate of each species which is replenished during the charging phase. We may describe the system dynamics with the following nine coupled differential equations:

$$\frac{dG_1}{dT} = \frac{G_1^m(T) - E(T)G_1(T)}{V}$$

$$\frac{dG_2}{dT} = \frac{G_2^m(T) - E(T)G_2(T)}{V}$$

$$\frac{dG_3}{dT} = \frac{G_3^m(T) - E(T)G_3(T)}{V}$$

$$\frac{dP_1}{dT} = \beta_1 H(T) S_1(T) \max(0, G_1(T) - P_3(T)) - \frac{E(T)P_1(T)}{V}$$

$$\frac{dP_2}{dT} = \beta_2 H(T) S_2(T) \max(0, G_2(T) - P_1(T)) - \frac{E(T)P_2(T)}{V}$$

$$\frac{dP_3}{dT} = \beta_3 H(T) S_3(T) \max(0, G_3(T) - P_2(T)) - \frac{E(T)P_3(T)}{V}$$

$$\frac{dS_1}{dT} = \frac{S_1^m(T)}{V} - \beta_1 H(T) S_1(T) \max(0, G_1(T) - P_3(T)) - \frac{E(T)S_1(T)}{V}$$

$$\frac{dS_2}{dT} = \frac{S_2^m(T)}{V} - \beta_2 H(T) S_2(T) \max(0, G_2(T) - P_1(T)) - \frac{E(T)S_2(T)}{V}$$

$$\frac{dS_3}{dT} = \frac{S_3^m(T)}{V} - \beta_3 H(T) S_3(T) \max(0, G_3(T) - P_2(T)) - \frac{E(T)S_3(T)}{V}$$

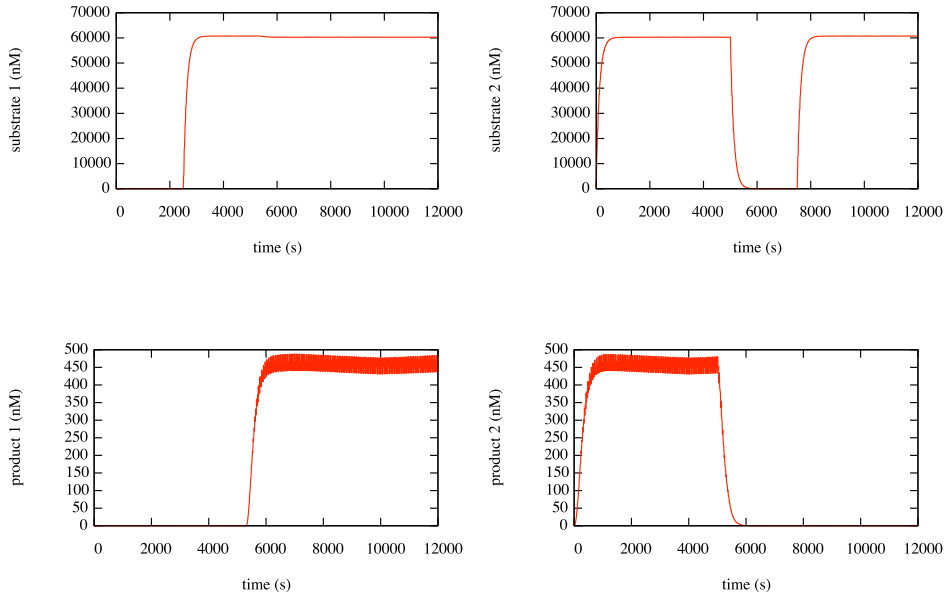

Figure 4: The flip-flop moved from set, to hold, to reset commands at 2500 s intervals.

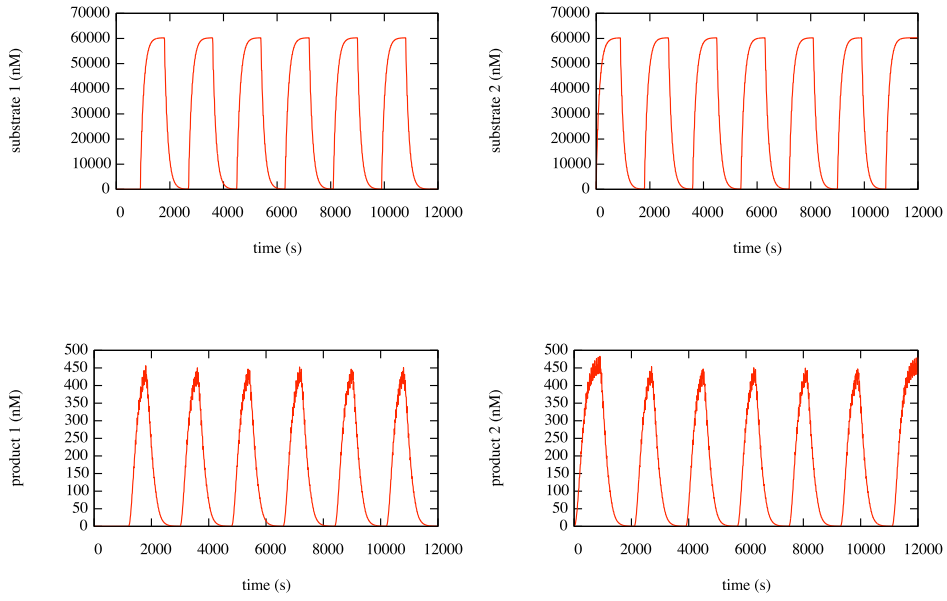

Figure 5: The flip-flop operating at its maximum switching speed.

where β_1, β_2, and β_3 are the reaction rate constants, V is the volume of the reactor, $E(T)$ is the time-dependent volumetric efflux, and $H(T)$ is the fraction of the reaction chamber which is homogeneous at time T.

The conditions under which the oscillator will oscillate in a CSTR have been examined previously [5]. To simplify things, this examination assumed that the concentration of substrate molecules in the chamber was constant, because, although these concentrations do oscillate, they are always much higher than the oscillating concentrations of the products. Using this assumption, linear approximations can be made to explicitly solve the differential equations for the oscillating product concentrations. These approximations give us a way to specify the center and period of the oscillations by setting an appropriate influx of substrate molecules and an appropriate concentration of gates. Our circumstances differ from the CSTR in that the efflux alternates between off and on, and the system is almost never completely homogeneous. We recognize that the system is never less than 76% homogeneous at any given time, however, and so it is reasonable to assume constant, complete homogeneity, and constant efflux, in order to use the approximation from our previous work as a starting point for specifying the period and center of the oscillator.

We set the efflux rate for the charging cycle equal to the rate we used for the flip-flop, $0.12\,\mathrm{nL\,s^{-1}}$. We use the same period (15 seconds in the charging phase and 15 seconds in the mixing phase) which worked well for the flip-flop. Based on the efflux rate, we use the linear approximations derived from the CSTR simulation research to calculate an estimate for the gate concentration and substrate influx needed for oscillations of period 250 seconds, centered at $1\,\mu$M. We find we should keep each of the gate concentrations steady at 1500 nM, while the molecular influx for each substrate should be set to $7.29 \times 10^{-6}\,\mathrm{nM\,s^{-1}}$. Figure 6 shows the results of integration over a 5000 second period with these initial values. We can see that the actual period is 480 seconds, and the actual center is close to $1.5\,\mu$M. The linear approximations were off by about 20% in the CSTR simulation; in our simulation, the period estimation is just over half the actual period, and the center estimation is off by about 50%. There are two reasons for this. One is the fact that we assumed our efflux rate and reactor homogeneity to be constant in order to use the same approximations that worked in the CSTR setting. Another, more instrumental reason stems from the fact that reactions happen much more quickly in our microfluidic system, since we have a much higher concentration of reagents. This causes the nonlinear terms that are not taken into account in the linear approximations to become much more prominent. More analysis is required to find a more accurate way to specify the period and center of our oscillations.

7 Related Work

Microfluidics has previously been proposed as a laboratory implementation technique for automating DNA-based combinatorial computation algorithms [9–11]. McCaskill and van Noort have solved the maximum clique graph problem for a 6-node graph in the lab using microfluidic networks and DNA [12–14]. Their approach uses DNA not as an enzyme but as an easily selectable carrier of information (using Watson-Crick base pair matching). The computational network which solves the maximum clique problem requires a large number of microchannels, proportional to the number of gates in the system, which grows as the number of graph nodes squared. Our approach, in contrast, may allow one to implement complex logic, performed with multiple types of gates, inputs, and products, in a single reaction chamber, in addition to allowing the possibility of linking several chambers together. Recently, van Noort and McCaskill have discussed systematic flow pattern solutions in support of microfluidic network design [15]; it remains to be seen if these techniques can be extended to handle designs such as ours.

Other work shows that it is even possible to use microfluidics for computational purposes as a purely mechanical substrate, i.e., without chemical reactions [16–18]. That fluidics can be used thus has been known for a long time [19], but microfluidics for the first time offers the potential for building relatively complex devices [20–22].

Microfluidic mixing is a difficult problem. While we have opted for the rotary mixing chamber design as one for which modeling the kinetics of mixing is within reach, other designs have been proposed;

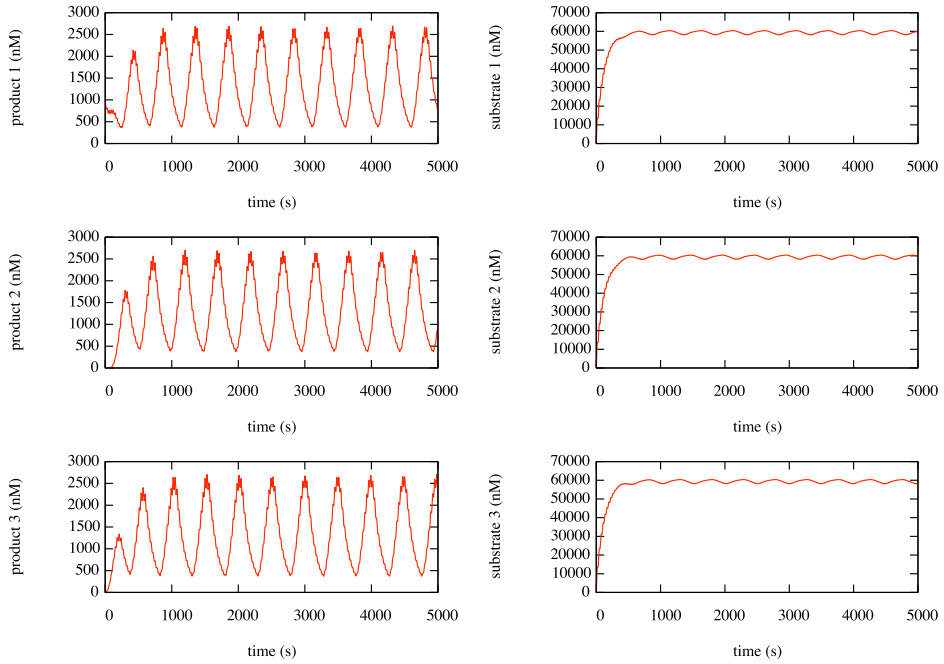

Figure 6: The oscillator system operating with a period of 480 s and a center of 1.5 μM.

droplet-based mixing [23–25] is especially attractive [26]. Analysis of mixing remains a challenging problem [27, 28]. Related to mixing, or achieving uniform concentration, is the problem of achieving particular spatiotemporally nonuniform concentrations [29–31].

Numerous oscillatory chemical and biochemical processes have been reported in the past decades, starting with the famous Belousov-Zhabotinsky reaction [32–35], via studies of hypothetical systems of coupled chemical reactions (some even intended as computational devices) [36–44], to the recent remarkable demonstration by Elowitz and Leibler of a gene transcription oscillatory network [45].

8 Conclusions

Networks of deoxyribozyme-based logic gates can function correctly in a microfluidic environment. This is the first feasible setting in which open-reactor experiments using these gates may be conducted in the laboratory. The immediate and obvious advantage of this approach, compared to using a larger open reactor, is a massive savings of cost and time. Our simulations of a flip-flop and an oscillator in such a setting show that useful microfluidic experiments could be conducted in mere hours, rather than the days or weeks it would take to see results in a large, continuous-flow stirred tank reactor. Perhaps most significantly, the extremely small volume of a microfluidic reactor means that a three-hour experiment could cost less than $50 in reagents, even though deoxyribozyme-based gates and the oligonucleotide substrates and inputs which they react with can cost as much as $40 per nanomole. The materials cost for the flip-flop experiment can thus be around $1,000; the cost of microfluidic chip fabrication is estimated at $20,000 [S. Han, personal communication], assuming an existing facility.

Our microfluidic reaction chambers are also very conducive to being networked together, with control logic outside the system operating valves on the channels connecting them. We will investigate the possibility of attaching gate molecules to beads, and keeping them within a chamber by placing semipermeable membranes at the chamber entrances and exits. With such a system, we could keep discrete sections of logic separate from each other when desired, and redirect outputs and inputs selectively.

This may be especially useful if certain types of gates whose logic we wish to connect actually conflict undesirably with each other if they are placed in the same chamber (by partially binding to each others' input or substrate molecules, for example). We believe that using microfluidic rotary mixing chambers to implement complex logic with deoxyribozyme-based gates in actual laboratory experiments is the first step toward completely understanding their potential, and eventually even deploying them in situations as complex as living cells.

9 Acknowledgments

We are grateful to Plamen Atanassov, Sang Han, Elebeoba May, Sergei Rudchenko, and Milan Stojanovic for helpful advice, to Clint Morgan for his simulation code, and to the anonymous reviewers for their detailed comments, and especially for alerting us to the work of van Noort. This material is based upon work supported by the National Science Foundation (grants CCR-0219587, CCR-0085792, EIA-0218262, EIA-0238027, and EIA-0324845), Sandia National Laboratories, Microsoft Research, and Hewlett-Packard (gift 88425.1). Any opinions, findings, and conclusions or recommendations expressed in this material are those of the author(s) and do not necessarily reflect the views of the sponsors.

References

[1] Milan N. Stojanovic, Tiffany Elizabeth Mitchell, and Darko Stefanovic. Deoxyribozyme-based logic gates. *Journal of the American Chemical Society*, 124(14):3555–3561, April 2002.

[2] Milan N. Stojanovic and Darko Stefanovic. Deoxyribozyme-based half adder. *Journal of the American Chemical Society*, 125(22):6673–6676, 2003.

[3] Milan N. Stojanovic and Darko Stefanovic. A deoxyribozyme-based molecular automaton. *Nature Biotechnology*, 21(9):1069–1074, September 2003.

[4] Milan N. Stojanovic, Stanka Semova, Dmitry Kolpashchikov, Joanne Macdonald, Clint Morgan, and Darko Stefanovic. Deoxyribozyme-based ligase logic gates and their initial circuits. *Journal of the American Chemical Society*, 2005. (in press).

[5] Clint Morgan, Darko Stefanovic, Cristopher Moore, and Milan N. Stojanovic. Building the components for a biomolecular computer. In *DNA Computing: 10th International Meeting on DNA-Based Computers*, 2004.

[6] Hou-Pu Chou, Marc A. Unger, and Stephen R. Quake. A microfabricated rotary pump. *Biomedical Microdevices*, 3(4):323–330, 2001.

[7] Marc A. Unger, Hou-Pu Chou, Todd Thorsen, Axel Scherer, and Stephen R. Quake. Monolithic microfabricated valves and pumps by multilayer soft lithography. *Science*, 298:580–584, 2000.

[8] John Crank. *The Mathematics of Diffusion*. Oxford University Press, second edition, 1975.

[9] Michael S. Livstone and Laura F. Landweber. Mathematical considerations in the design of microreactor-based DNA computers. In *DNA Computing: 9th International Meeting on DNA-Based Computers*, volume 2943 of *Lecture Notes in Computer Science*, pages 180–189, Madison, Wisconsin, June 2003. Springer-Verlag.

[10] Ashish Gehani and John Reif. Micro-flow bio-molecular computation. *BioSystems*, 52(1–3), October 1999.

[11] Lucas Ledesma, Daniel Manrique, Alfonso Rodríguez-Patón, and Andrés Silva. A tissue P system and a DNA microfluidic device for solving the shortest common superstring problem.

[12] Danny van Noort, Frank-Ulrich Gast, and John S. McCaskill. DNA computing in microreactors. In *DNA Computing: 7th International Meeting on DNA-Based Computers*, 2001.

[13] Patrick Wagler, Danny van Noort, and John S. McCaskill. Dna computing in microreactors. *Proceedings of SPIE*, 4590:6–13, November 2001.

[14] Danny van Noort, Patrick Wagler, and John S. McCaskill. Hybrid poly(dimethylsoloxane)-silicon microreactors used for molecular computing. *Smart Materials and Structures*, 11:756–760, 2004.

[15] Danny van Noort and John S. McCaskill. Flows in micro fluidic networks: From theory to experiment. *Natural Computing*, 3(4):395–410, 2004.

[16] Daniel T. Chiu, Elena Pezzoli, Hongkai Wu, Abraham D. Stroock, and George M. Whitesides. Using three-dimensional microfluidic networks for solving computationally hard problems. *Proceedings of the National Academy of Sciences of the USA*, 98(6):2961–2966, March 2001.

[17] Michael J. Fuerstman, Pascal Deschatelets, Ravi Kane, Alexander Schwartz, Paul J. A. Kenis, John M. Deutsch, and George M. Whitesides. Solving mazes using microfluidic networks. *Langmuir*, 19:4714–4722, 2003.

[18] Tor Vestad, David W. M. Marr, and Toshinori Munakata. Flow resistance for microfluidic logic operations. *Applied Physics Letters*, 84(25):5074–5075, June 2004.

[19] Keith Foster and Graham A. Parker, editors. *Fluidics: components and circuits*. Wiley-Interscience, London and New York, 1970.

[20] Todd Thorsen, Sebastian J. Maerkl, and Stephen R. Quake. Microfluidic large-scale integration. *Science*, 298:580–584, 2002.

[21] Alex Groisman, Markus Enzelberger, and Stephen R. Quake. Microfluidic memory and control devices. *Science*, 300:955–958, 2003.

[22] Jong Wook Hong and Stephen R. Quake. Integrated nanoliter systems. *Nature Biotechnology*, 21:1179–1183, 2003.

[23] Phil Paik, Vamsee K. Pamula, and Richard B. Fair. Rapid droplet mixers for digital microfluidic systems. *Lab on a Chip*, 3:253–259, 2003.

[24] Joshua D. Tice, Helen Song, Adam D. Lyon, and Rustem F. Ismagilov. Formation of droplets and mixing in multiphase microfluidics at low values of the Reynolds and the capillary numbers. *Langmuir*, 19:9127–9133, 2003.

[25] Helen Song, Joshua D. Tice, and Rustem F. Ismagilov. A microfluidic system for controlling reaction networks in time. *Angewandte Chemie International Edition*, 42:768–772, 2003.

[26] Cory J. Gerdts, David E. Sharoyan, and Rustem F. Ismagilov. A synthetic reaction network: Chemical amplification using nonequilibrium autocatalytic reactions coupled in time. *Journal of the American Chemical Society*, 126:6327–6331, 2004.

[27] Stephen Wiggins. Integrated nanoliter systems. *Nature Biotechnology*, 21:1179–1183, 2003.

[28] T. H. Solomon and Igor Mezić. Uniform resonant chaotic mixing in fluid flows. *Nature*, 425:376–380, September 2003.

[29] Noo Li Jeon, Stephan K. W. Dertinger, Daniel T. Chiu, Insung S. Choi, Abraham D. Stroock, and George M. Whitesides. Generation of solution and surface gradients using microfluidic systems. *Langmuir*, 16:8311–8316, 2000.

[30] Stephan K. W. Dertinger, Daniel T. Chiu, Noo Li Jeon, and George M. Whitesides. Generation of gradients having complex shapes using microfluidic networks. *Analytical Chemistry*, 73:1240–1246, 2001.

[31] Noo Li Jeon, Harihara Bakaran, Stephan K. W. Dertinger, Goerge M. Whitesides, Livingston Van De Water, and Mehmet Toner. Neutrophil chemotaxis in linear and complex gradients of interleukin-8 formed in a microfabricated device. *Nature Biotechnology*, 20:826–830, 2002.

[32] R. J. Field, E Körös, and R. Noyes. Oscillations in chemical systems. II. Thorough analysis of temporal oscillation in the bromate-cerium-malonic acid system. *Journal of the American Chemical Society*, 94:8649–8664, 1972.

[33] R. Noyes, R. J. Field, and E Körös. Oscillations in chemical systems. I. Detailed mechanism in a system showing temporal oscillations. *Journal of the American Chemical Society*, 94:1394–1395, 1972.

[34] John J. Tyson. *The Belousov-Zhabotinskii Reaction*, volume 10 of *Lecture Notes in Biomathematics*. Springer-Verlag, Berlin, 1976.

[35] Irving R. Epstein and John A. Pojman. *An Introduction to Nonlinear Chemical Dynamics*. Oxford University Press, New York, 1998.

[36] Allen Hjelmfelt and John Ross. Chemical implementation and thermodynamics of collective neural networks. *Proceedings of the National Academy of Sciences of the USA*, 89(1):388–391, January 1992.

[37] A. Hjelmfelt and J. Ross. Pattern recognition, chaos, and multiplicity in neural networks of excitable systems. *Proceedings of the National Academy of Sciences of the USA*, 91(1):63–67, January 1994.

[38] A. Hjelmfelt, F. W. Schneider, and J. Ross. Pattern recognition in coupled chemical kinetic systems. *Science*, 260:335–337, April 1993.

[39] Allen Hjelmfelt, Edward D. Weinberger, and John Ross. Chemical implementation of neural networks and Turing machines. *Proceedings of the National Academy of Sciences of the USA*, 88(24):10983–10987, December 1991.

[40] Allen Hjelmfelt, Edward D. Weinberger, and John Ross. Chemical implementation of finite-state machines. *Proceedings of the National Academy of Sciences of the USA*, 89(1):383–387, January 1992.

[41] Jean-Pierre Laplante, Maria Pemberton, Allen Hjelmfelt, and John Ross. Experiments on pattern recognition by chemical kinetics. *The Journal of Physical Chemistry*, 99(25):10063–10065, June 1995.

[42] O. E. Rössler. A principle for chemical multivibration. *Journal of Theoretical Biology*, 36:413–417, 1972.

[43] Otto E. Rössler and Friedrich F. Seelig. A Rashevsky-Turing system as a two-cellular flip-flop. *Zeitschrift für Naturforschung*, 27 b:1444–1448, 1972.

[44] Friedrich F. Seelig and Otto E. Rössler. Model of a chemical reaction flip-flop with one unique switching input. *Zeitschrift für Naturforschung*, 27 b:1441–1444, 1972.

[45] Michael B. Elowitz and Stanislas Leibler. A synthetic oscillatory network of transcriptional regulators. *Nature*, 403:335–338, January 2000.